Materials Research. 2023; 26(suppl.1):e20230080
DOI: https://doi.org/10.1590/1980-5373-MR-2023-0080

Alternative Sample Preparation of Co-28Cr-6Mo to Avoid Strain-induced Phase Transformation

I. S. Cesarin[a], L.H.M. Antunes[a], G. Darin Filho[b], C. Ulsen[c], P.F.S. Farina[a]*

[a]*Universidade Estadual de Campinas (UNICAMP), Faculdade de Engenharia Mecânica, Rua Mendeleyev, 200, 13083- 860, Campinas, SP, Brasil.*
[b]*Universidade de São Paulo (USP), Escola Politécnica, Laboratório de Caracterização Tecnológica, Av. Prof. Mello Moraes, 2373, 05508-030, São Paulo, SP, Brasil.*
[c]*Universidade de São Paulo (USP), Escola Politécnica, Departamento de Engenharia de Minas e de Petróleo, Av. Prof. Mello Moraes, 2373, 05508-030, São Paulo, SP, Brasil.*

Received: January 15, 2023; Revised: April 29, 2023; Accepted: June 18, 2023

The allotropic transformation, characteristic of cobalt-based alloys, occurs at around 970 ºC in Co-28Cr-6Mo alloys. When subjected to fast cooling, such alloys can maintain the high temperature cubic centered phase at room temperature, resulting in a CFC metastable matrix. This metastable condition leads to a nucleation of the hexagonal phase (the stable one), which is induced by deformation or isothermally. In general, Co-based alloys are submitted to solution heat treatment plus aging to control both the precipitation of carbides and the nucleation of the hexagonal phase. When the study of this type of alloy is conducted in the metastable condition, it is extremely important do not induce the hexagonal phase during sample preparation. Traditionally, the metallographic route preparation is carried out using electropolishing to avoid the deformation-induced phase transformation. The need for specialized equipment and hazardous electrolytes to perform electropolishing limits its use. Therefore, the aim of the present work is to propose the use of an adaptation to traditional metallographic techniques in order to prepare Co-28Cr-6Mo alloy samples. To this end, the samples prepared by three different routes were analyzed by X-Ray diffraction, including Rietveld refinement, as well as EBSD in order to identify and quantify the phases present in the structure. A control cold rolled sample was also analyzed. The results showed a significant reduction in the HCP phase fraction, strain-induced during grinding, after the application of the alternative preparation method proposed. Further studies might be useful to validate the present methodology.

Keywords: *sample preparation, metallography, XRD, Rietveld, EBSD.*

1. Introduction

ASTM F75 alloys (Co-28Cr-6Mo) have been extensively used as an implant material in orthopedics and dentistry due to its biocompatibility and mechanical and wear resistance[1]. At room temperature, such alloys are single-phase, being composed of a hexagonal closed packed (HCP) phase called ε-HCP. An important feature of cobalt-based alloys is the polymorphic transformation that occurs at around 970 ºC in the F75 alloy[2]. During this transformation, the high temperature face-centered cubic (FCC) phase known as γ-FCC transforms into ε-HCP phase under slow cooling. However, if fast cooling is applied, the γ-FCC phase can occur at room temperature in a metastable condition. From the metastable γ-FCC phase, it is possible to obtain the ε-HCP phase both under an isothermal heat treatment at around 800 ºC [3] and by the strain-induced martensitic transformation (SIMT)[4].

Cobalt-based alloys are traditionally applied after solubilization and aging heat treatments. Solubilization is used to dissolve coarse carbides from the casting process and precipitate fine carbides, while aging produces the ε-HCP phase isothermally[5], resulting in an ε-HCP matrix with dispersed fine carbides.

Recently, the use of additive manufacturing (AM) to produce orthopedic and dental implants has been gaining relevance. The possibility of obtaining implants customized for each patient and designed to achieve the best performance of osseointegration and mechanical behavior has attracted a lot of attention in the field of AM technology. Among the available techniques of metal AM, laser powder bed fusion (L-PBF) stands out. Such technique consists of laser melting micrometric layers of metallic powder which are deposited and melted successively on each other until the piece is obtained in its final shape.

The high intensity of the incident laser beam focused on an area of approximately 100 microns has enough energy to melt the metallic powder. The surrounding metallic powder acts as a heat conductor, quickly dissipating heat and cooling the molten region, resulting in a single-phase γ-FCC matrix. Moreover, the studied alloy presents a relatively high carbon and nitrogen content (0.14 and 0.13 wt%, respectively). It was shown that carbon and nitrogen stabilize the γ-FCC phase and suppress the athermal martensitic transformation[6,7], forming a single-phase γ-FCC structure identified as "as-built".

* e-mail: lhmantunes@gmail.com

Therefore, the study of such alloys relies on the metastable condition in which only the γ-FCC phase is present. In this way, it becomes necessary to understand more accurately the effects of thermal treatments, especially the precipitation of the ε-HCP phase.

Due to SIMT, special attention should be given to the metallographic preparation of such metastable samples. The presence of a metastable phase combined with the residual stress resulting from the solidification of each layer favors the occurrence of the strain-induced ε-HCP phase[8]. The grinding step of the metallographic preparation process may be sufficient to induce this stable phase. In order to avoid SIMT, some authors[9-11] have proposed some alternatives for sample preparation. The most used technique is electropolishing, which consists of applying a voltage to the sample and putting it into contact with an electrolyte. Although this process chemically removes the surface layer of the sample, it requires specific equipment and may be dangerous depending on the electrolyte used. Thus, electropolishing is restricted to well-equipped laboratories and should be performed by trained operators.

In this context, the present work aims to verify the effect of manual grinding and polishing during the preparation of ASTM F75 Co-based alloys on the SIMT in comparison with an electropolished sample (single-phase CFC) and a cold rolled electropolished sample (CFC + HCP phases).

2. Experimental Procedure

The alternative sample preparation proposed herein is based on the traditional metallography, i.e., grinding and polishing, with the addition of a more precise polishing step using VibroMet™. Such equipment is comprised of a polishing cloth soaked in an alumina or silica suspension with very fine grain size. Sample holders made of ferromagnetic stainless steel hold the samples and press them against the polishing cloth with their own weight. Finally, a magnetic base underneath the polishing cloth vibrates and rotates, consequently moving the samples. This vibrational motion gives a uniform and precise polished finish to the samples.

To evaluate the effect of manual grinding and polishing during the metallographic preparation of samples, a methodology capable of ensuring the reliability and reproducibility of the experiment as well as the integrity of the sample was elaborated. Plates with 12 x 6 x 3 mm3 were produced by L-PBF using MP1 Co-Cr-Mo metallic powder feedstock, supplied by EOS GmbH. The chemical composition (wt%) of the produced samples was determined by X-ray fluorescence and the carbon and nitrogen contents were obtained by combustion infrared detection and inert gas fusion, respectively: 27.89Cr–6.27Mo–0.72Mn–0.62Si–0.32Fe–0.1Ni–0.14C–0.13N, with balance Co.

Each additively manufactured plate had its metallographic preparation process interrupted at different stages, as follows:

- G - Grinded
- GP - Grinded + Polished
- GPV - Grinded + Polished + VibroMet™
- CRGPV - Cold Rolled + Grinded + Polished + VibroMet™

In the "G" condition, only grinding was performed with 100, 220, 320, 400, 600, 800, 1200 1500 and 2000 grit emery paper. The "GP" condition stands for grinding followed by polishing with an alumina suspension of 1 μm and 0.3 mμ for 5 minutes each. In the "GPV" condition, the metallographic process was complete, i.e., besides grinding and polishing, an additional polishing step using a Buehler VibroMet™ polisher was performed with a colloidal silica suspension of 0.04 μm for 12 hours. Finally, the "CRGPV" condition was used as a control, ensuring the presence of the ε-HCP phase in its structure. In this condition, the sample was cold rolled at a 20% reduction, and subsequently prepared following the same steps of the GPV condition.

The crystalline phases of each sample were determined by X-ray diffraction (XRD) to confirm the occurrence of the γ-FCC and ε-HCP phases during each step of sample preparation. The XRD patterns were obtained using Cu Ka radiation and an Empyrean diffractometer (Panalytical) operating in the Bragg-Brentano configuration. Table 1 lists the parameters used to acquire the diffractograms.

To quantify the phases present in the sample, a refinement of the crystalline structures was carried out using the Rietveld refinement method. This method involves the minimization of the residual function of a nonlinear least-squares algorithm to refine the crystalline structure of a compound. In this work, the Highscore Plus 4.0 software was used to adjust the XRD diffractogram, and therefore quantify the γ-FCC and ε-HCP phases after each step of the metallographic preparation. The strategy for refinement was based on Young's guidelines[12], and the results became acceptable when the convergence of statistical parameters reached values compatible with Hill and Flack criteria[13]. In addition to the Rietveld refinement, a quantification of the phases was performed via backscatter electron diffraction (EBSD). Since this technique requires a great quality of surface preparation to guarantee the indexing of Kikuchi lines, only the GPV and CRGPV conditions were analyzed.

The microstructures of the samples were characterized by scanning electron microscopy on a Thermo Scientific/FEI Quanta 650 microscope with an EBSD detector. The EBSD maps were acquired using the AZtecHKL software and processed with the HKL Channel 5 software package, both from Oxford Instruments.

Table 1. X-ray diffraction parameters.

X-ray Tube	Voltage (kV)	Current (mA)	Starting angle (º)	Final angle (º)	Angular step (º)	Time per step (s)
Cu	45	40	35.0	90.0	0.02	5.0

3. Results and Discussion

The diffractograms obtained from the X-ray diffraction analysis are shown in Figure 1. The diffraction peaks were indexed to the FIZ Karlsruhe's Inorganic Crystal Structure Database (ICSD) under the codes 98-006-1642 for the γ-FCC phase and 98-06-2984 for the ε-HCP phase. It is noticeable that the grinding (G) process induces the formation of the ε-HCP phase, and as the metallographic process progresses with polishing (GP) and the use of VibroMet™ (GPV), the ε-HCP peaks lose intensity, indicating a reduction in the phase fraction.

The angular range proved to be adequate to perform the Rietveld refinement. As observed, peaks at larger 2θ angles have lower angular resolution, which hampers the Rietveld refinement. For the Rietveld simulation, three peaks of the FCC phase were considered: (111), (200) and (220). When both γ-FCC and ε-HCP phases were present, six additional peaks were analyzed: $(10\bar{1}0)$, (0002), $(10\bar{1}1)$, $(10\bar{1}2)$, $(11\bar{2}0)$ and $(10\bar{1}3)$. The parameters used for the simulation included background, scale factor, unit cell parameters, preferential orientation, peak shape and peak profile. The main results can be seen in Table 2.

The low variation in the lattice parameter is within the expected range due to the sample preparation methods used. All indices are in accordance with the acceptable limits reported in the literature[13]. The FCC peak broadening, observed in the G and CRGPV samples is related to microstrains in the crystal lattice. Since there is an increase in volume when CFC to HCP phase transformation occurs, some deformation also occurs at the surrounding CFC austenite due to the plastic accommodation of the shape deformation[14,15].

The band contrast images in Figures 2b and d illustrate the typical microstructure of the Co-28Cr-6Mo alloy when produced by L-PBF, consisting of elongated grains parallel to the heat transfer direction during cooling[16-18]. In Figure 2d, a greater number of slip bands can be noted. As reported in the literature, stacking faults, abundantly found in highly deformed materials, are preferential sites for the ε-HCP phase nucleation[15,19]. This justifies the higher volume fraction of the ε-HCP phase observed in the CRGPV specimen (Figures 2c and 3).

In the chart of Figure 3, the proportions of each phase determined by Rietveld refinement and EBSD are presented. According to the Rietveld refinement results, there was a reduction in the amount of the ε-HCP phase from 27.4 to near 0% as steps were added to the metallographic preparation process, while the EBSD analysis revealed that GPV sample was comprised of 0.4% of the ε-HCP phase. In relation to the CRGPV sample, both techniques pointed to the presence of around 29% of this phase.

It was observed that traditional metallographic preparation by manual grinding induces the ε-HCP phase through the SIMT process occurring on the surface of the samples. However, subsequent polishing steps and VibroMet™ act by removing this surface layer smoothly, without promoting SIMT.

The GPV sample presented an amount of 0.0 and 0.4% of the ε-HCP phase, while the CRGPV sample was comprised of 27.6 and 29.8% of this phase, according to the Rietveld refinement and EBSD analyses, respectively. The small difference observed in the GPV sample confirms that the ε-HCP phase fraction present in this sample is close to zero. When dealing with small amounts of phases, e.g., below 2%, the Rietveld refinement technique may produce unprecise results. Therefore, even though a complete absence of the ε-HCP phase was noticed, this may not be entirely true. On the other hand, the 2.2% difference observed in the CRGPV sample between the Rietveld and EBSD results may be attributed to unindexed regions in the EBSD phase map.

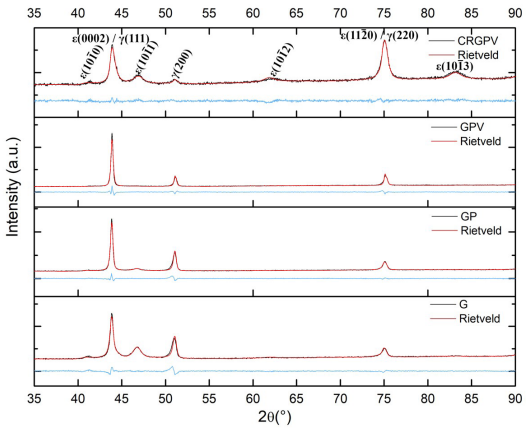

Figure 1. Diffractograms of the four conditions analyzed (black curve) with refinement overlap (red line).

Table 2. Results of parameters refined using the Rietveld method.

Sample	Lattice parameter g-FCC	Lattice parameter e-HCP	R_{wp} (%)	GoF (%)	R_{exp} (%)
G	a=3.5842(3)Å	a=2.5567(5)Å c=4.0912(4)Å	6.74	1.83	3.68
GP	a=3.5817(2)Å	a=2.5535(2)Å c=4.1069(3)Å	6.91	1.66	4.17
GPV	a=3.5759(1)Å		7.6	1.82	4.17
CRGPV	a=3.5869(2)Å	a=2.5463(3)Å c=4.1074(2)Å	4.87	1.31	3.71

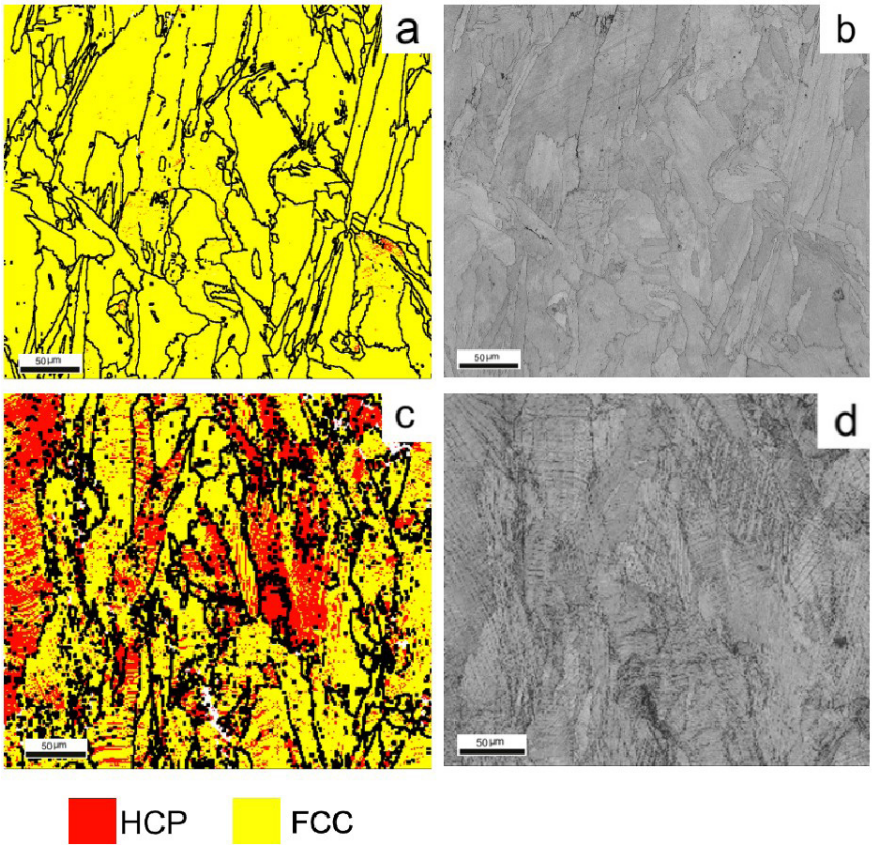

Figure 2. a) and c) Phase maps of the GPV and CRGPV samples, respectively; and b) and d) band contrast of the GPV and CRGPV samples, respectively.

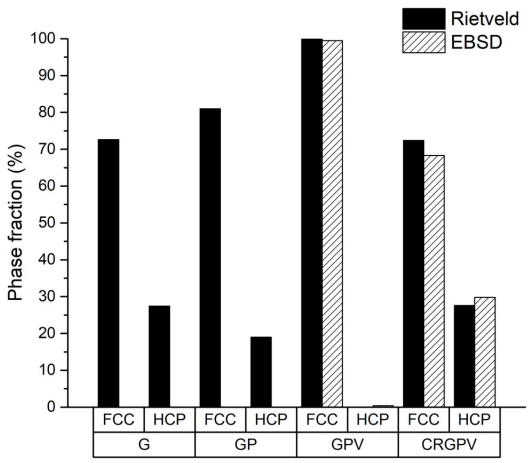

Figure 3. Values of phase quantification analyses by Rietveld refinement and EBSD.

Due to the cold rolling process, highly deformed regions are formed, making crack nucleation not uncommon. Thus, it can be concluded that unindexed regions such as the white ones in Figure 2c increases the uncertainty of the volume fraction of the ε-HCP phase obtained from the EBSD analysis.

As already mentioned, although the ε-HCP phase percentage verified in the GPV sample is small, it does not guarantee the total absence of this phase in the sample. For studies and applications that use aged samples, i.e., with a fraction of the ε-HCP phase being obtained isothermally, the possible presence of this phase due to the SIMT process induced by grinding may not have a relevant effect on the performance of the material. Nevertheless, when one wishes to study or apply the alloy in its metastable condition, that is, only with the γ-FCC phase, it is preferable to perform electropolishing, either as the only preparation step or as a final step, after manual polishing.

4. Conclusions

The results obtained herein referring to the metallographic preparation indicated that grinding superficially induces the formation of the hexagonal phase (ε-HCP) through the SIMT mechanism. Both the polishing technique and the use of VibroMet™ were able to significantly reduce the induced phase, which at the end of the entire process achieved approximately 0.4% of remaining ε-HCP.

For applications where the alloy is submitted to aging and is comprised of the isothermal ε-HCP phase, the metallographic preparation proposed in this work can be successfully employed. However, electropolishing is recommended for studies and applications in which one wishes to work with a fully γ-FCC structure.

5. Acknowledgments

The authors are grateful to INCT Biofabris for the assistance provided with the manufacturing of the specimens and LCT-USP for performing part of the experimental analysis. We also acknowledge the experimental support by F. E. Montoro at the Brazilian Nanotechnology National Laboratory (project SEM–C1–26162) and M. Béreš at the Analytical Center of UFC/CT-INFRA/MCTI-SISNANO. This study was financed by the Coordination for the Improvement of Higher Education Personnel (CAPES), Brazil (Finance Code 001).

6. References

1. Chen Q, Thouas GA. Metallic implant biomaterials. Mater Sci Eng Rep. 2015;87:1-57.
2. Saldívar García ADJ, Medrano AM, Rodríguez AS, Salinas Rodríguez A. Formation of hcp martensite during the isothermal aging of an fcc Co-27Cr-5Mo-0.05C orthopedic implant alloy. Metall Mater Trans, A Phys Metall Mater Sci. 1999;30(5):1177-84.
3. Cai S, Daymond MR, Ren Y. Stress induced martensite transformation in Co–28Cr–6Mo alloy during room temperature deformation. Mater Sci Eng A. 2013;580:209-16.
4. Olson GB, Cohen M. A mechanism for the strain-induced martensitic transformations. J Less Common Met. 1972;28:107-18.
5. Bedolla-Gil Y, Hernandez-Rodriguez MAL. Tribological behavior of a heat-treated cobalt-based alloy. J Mater Eng Perform. 2013;22(2):541-7.
6. Lee SH, Takahashi E, Nomura N, Chiba A. Effect of heat treatment on microstructure and mechanical properties of Ni- and C-free Co-Cr-Mo alloys for medical applications. J JPN I Met Mater. 2005;70(4):260-4.
7. Song C, Park H, Seong H, López HF. Development of athermal and isothermal ε-martensite in atomized Co-Cr-Mo-C implant alloy powders. Metall Mater Trans, A Phys Metall Mater Sci. 2006;37(11):3197-204.
8. Béreš M, Silva CC, Sarvezuk PWC, Wu L, Antunes LHM, Jardini AL, et al. Mechanical and phase transformation behaviour of biomedical Co-Cr-Mo alloy fabricated by direct metal laser sintering. Mater Sci Eng A. 2018;714:36-42.
9. Wu W, Song M, Ni S, Wang J, Liu Y, Liu B, et al. Dual mechanisms of grain refinement in a FeCoCrNi highentropy alloy processed by highpressure torsion. Sci Rep. 2017;7:46720.
10. Seki E, Kajima Y, Takaichi A, Kittikundecha N, Cho HHW, Htat HL, et al. Effect of heat treatment on the microstructure and fatigue strength of CoCrMo alloys fabricated by selective laser melting. Mater Lett. 2019;245:53-6.
11. Lee BS, Koizumi Y, Matsumoto H, Chiba A. Collective behavior of strain-induced martensitic transformation (SIMT) in biomedical Co–Cr–Mo–N alloy polycrystal: an ex-situ electron backscattering diffraction study. Mater Sci Eng A. 2014;611:263-73.
12. Young RA. The rietveld method. Vol. 5. Chester, Cheshire: International Union of Crystallography; 1993.
13. Hill RJ, Flack HD. The use of the Durbin–Watson d statistic in Rietveld analysis. J Appl Cryst. 1987;20(5):356-61.
14. Miyamoto G, Shibata A, Maki T, Furuhara T. Precise measurement of strain accommodation in austenite matrix surrounding martensite in ferrous alloys by electron backscatter diffraction analysis. Acta Mater. 2009;57(4):1120-31. https://doi.org/10.1016/j.actamat.2008.10.050.
15. Antunes LHM, Hoyos JJ, Fonseca EB, Béreš M, da Silva Farina PF, Lopes ESN, et al. Effect of phase transformation on ductility of additively manufactured Co–28Cr–6Mo alloy: an *in situ* synchrotron X-ray diffraction study during mechanical testing. Mater Sci Eng A. 2019;764:138262. https://doi.org/10.1016/j.msea.2019.138262.
16. Wei HL, Mazumder J, DebRoy T. Evolution of solidification texture during additive manufacturing. Sci Rep. 2015;5(1):16446.
17. Lee HW, Jung KH, Hwang SK, Kang SH, Kim DK. Microstructure and mechanical anisotropy of CoCrW alloy processed by selective laser melting. Mater Sci Eng A. 2019;749:65-73.
18. Takaichi A, Suyalatu, Nakamoto T, Joko N, Nomura N, Tsutsumi Y, et al. Microstructures and mechanical properties of Co-29Cr-6Mo alloy fabricated by selective laser melting process for dental applications. J Mech Behav Biomed Mater. 2013;21:67-76.
19. Olson GB, Cohen M. A general mechanism of martensitic nucleation: part I. General concepts and the FCC → HCP transformation. Metall Trans, A, Phys Metall Mater Sci. 1976;7(12):1897-904.